Supplemental Information for:

Terrestrial sources as the primary delivery mechanism of mercury to the oceans across the Toarcian Oceanic Anoxic Event (Early Jurassic)

T.R. Them II[a,*], C.H. Jagoe[b], A.H. Caruthers[c], B.C. Gill[d], S.E. Grasby[e], D.R. Gröcke[f], R. Yin[g], and J.D. Owens[h,i]

[a]Department of Geology and Environmental Geosciences, College of Charleston, Charleston, SC 29424, USA
[b]School of the Environment, Florida A&M University, Tallahassee, FL 32307, USA.
[c]Department of Geosciences, Western Michigan University, Kalamazoo, MI 49006, USA.
[d]Department of Geosciences, Virginia Polytechnic Institute and State University, Blacksburg, VA 24061, USA.
[e]Geological Survey of Canada, Natural Resources Canada, Calgary, Alberta T2L 2A7, Canada.
[f]Department of Earth Sciences, Durham University, Durham, DH1 3LE, UK.
[g]State Key Laboratory of Ore Deposit Geochemistry, Institute of Geochemistry, Chinese Academy of Sciences, Guiyang 550002, China.
[h]Department of Earth, Ocean & Atmospheric Science, Florida State University, Tallahassee, FL 32306, USA.
[i]National High Magnetic Field Laboratory, Florida State University, Tallahassee, FL 32310, USA.

* Corresponding author: themtr@cofc.edu (T.R. Them II)

SUPPLEMENTAL INFORMATION

Thermal maturity of Gordondale, Red Deer, and Poker Chip Shale members in the Fernie Formation

It is imperative to account for the thermal maturity of the rock as Hg can be volatilized during burial diagenesis. For our section we can compare the outcrop section (East Tributary) to the drill cores (1-35-62-20W5 and 6-32-78-5W6). The East Tributary section has higher Hg contents when compared to the drill cores (Main Text, SI Data). These elevated Hg contents are most likely not due to differences in thermal maturity, as the outcrop section (exposed in western Alberta Rocky Mountains) experienced much higher temperatures than the drill cores (Reidiger et al., 1990; Reidiger, 1993, 2002; Kondla et al., 2017). Thus, the proximal to distal variation in Hg and Hg/TOC data is most likely due to other factors not related to the burial histories of these successions.

Standard and sample reproducibility

In the table below, we report international mercury standards used to calibrate the data at Florida A&M University that were all run at least four times.

Table S2. Error analysis

Standard	Hg Contents (mg/kg)	Number of Analyses	2-sigma Standard Deviation (± mg/kg)	Accepted value (mg/kg)
SRM Spinach 1570a	0.0286	7	0.003	0.0297
SRM Mussel 2976	0.0620	7	0.005	0.061
TORT-2 SRM	0.2829	4	0.008	0.27
BCR-60 Aquatic Plant	0.3244	4	0.012	0.34

Additionally, we replicated 14 of our geological samples at least two times, and the average 2-sigma standard deviation of these replicate analyses is ± 0.005 ppm (5 ppb), with a rage of 0.000 to 0.018 ppm (0 to 18 ppb). Thus, we cannot attribute the Hg or Hg/TOC anomalies in samples that we have presented here as a result of analytical error with the Hg analyses.

Carbon, sulfur, and mercury relationships in the Posidonia Shale

Marlstone

The low TOC contents in the Marlstone unit, except for the two organic-rich intervals, causes the observed Hg/TOC anomalies. These low-TOC samples are displayed in Figure 4 in the main text, but in a different color than the rest of the organic-rich intervals.

Oil Shale and Bituminous Shale

The one-point Hg and Hg/TOC increase in the T-OAE interval intriguing because it may represent an increase in volcanic activity. The Hg content of this sample, however, is most likely controlled by another factor, pyrite contents. This sample is associated with very high pyrite contents (pyrite sulfur = 5.7 wt. %; Them et al., 2018), which is much higher than the rest of the samples (see SI Fig. 1). Furthermore, the relationship between pyrite sulfur and mercury concentrations (R^2 = 0.78) from this study location is higher than that of total organic carbon (TOC) and mercury relationship (R^2 = 0.49). If this sample with high pyrite sulfur wt. % is removed from these plots, TOC:Hg values are more closely related (R^2 = 0.80) than S-pyrite:Hg (R^2 = 0.67). This suggests that in the South German Basin, the one-point increase in Hg contents is most likely controlled by increased S-pyrite content of the sample. The stronger relationship between TOC and Hg in the rest of the samples suggests that overall Hg content of the South German Basin is controlled by organic matter production and preservation. Regardless, based on these relationships

alone it is not possible to determine the dominant phase the Hg is hosted in the rest of these samples.

Mercury relationships in Pleistocene Mediterranean marine sediments

Mercury data generated Mediterranean Sea Pleistocene sediments (ODP Hole 974C; Gehrke et al., 2009) show variable Hg and Hg/TOC values (SI Fig. 2). These Hg contents are on the order of some ancient sedimentary Hg enrichments linked to massive volcanism. However, the Hg enrichments at this location are all driven by redox changes and low TOC values (Gehrke et al., 2009), not volcanism.

Ancient mercury anomalies linked to large-scale volcanism

Numerous studies have applied the Hg proxy to Phanerozoic extinctions and oceanic anoxic events (OAEs) associated with documented or hypothesized LIP emplacements and have noted contemporaneous [Hg] and/or Hg/TOC anomalies (see Table S1). These records include the Late Devonian Frasnian-Famennian (unnamed volcanic LIP; Racki et al., 2018), Late Ordovician (unnamed volcanic LIP; Jones et al., 2017; Gong et al., 2017), late Permian to early Triassic (Siberian Traps; Sanei et al., 2012; Grasby et al., 2013, 2016, 2017), end-Triassic (Central Atlantic Magmatic Province; Thibodeau et al., 2016; Percival et al., 2017), Pliensbachian-Toarcian (Karoo-Ferrar LIP; Percival et al., 2015, 2016; Fantasia et al., 2018; c.f., this study), and end-Cretaceous (Deccan Traps; Font et al., 2016, 2018; Sial et al., 2013, 2014, 2016) mass extinctions. Additionally, the Hg proxy has also been applied to intervals that contain less severe biological events: the Valanginian Weissert OAE (Paraná-Etendeka LIP; Charbonnier et al., 2017), the Hauterivian and Barremian episodes (Ontang Jova LIP; Charbonnier et al.,

2018), the Aptian/Albian OAE 1a (Ontang Jova LIP; Charbonnier and Föllmi, 2017), and Mid-Cenomanian Event and OAE 2 (Madagascan, Ontong-Java, Caribbean, and/or High Arctic LIPs; Scaife et al., 2017).

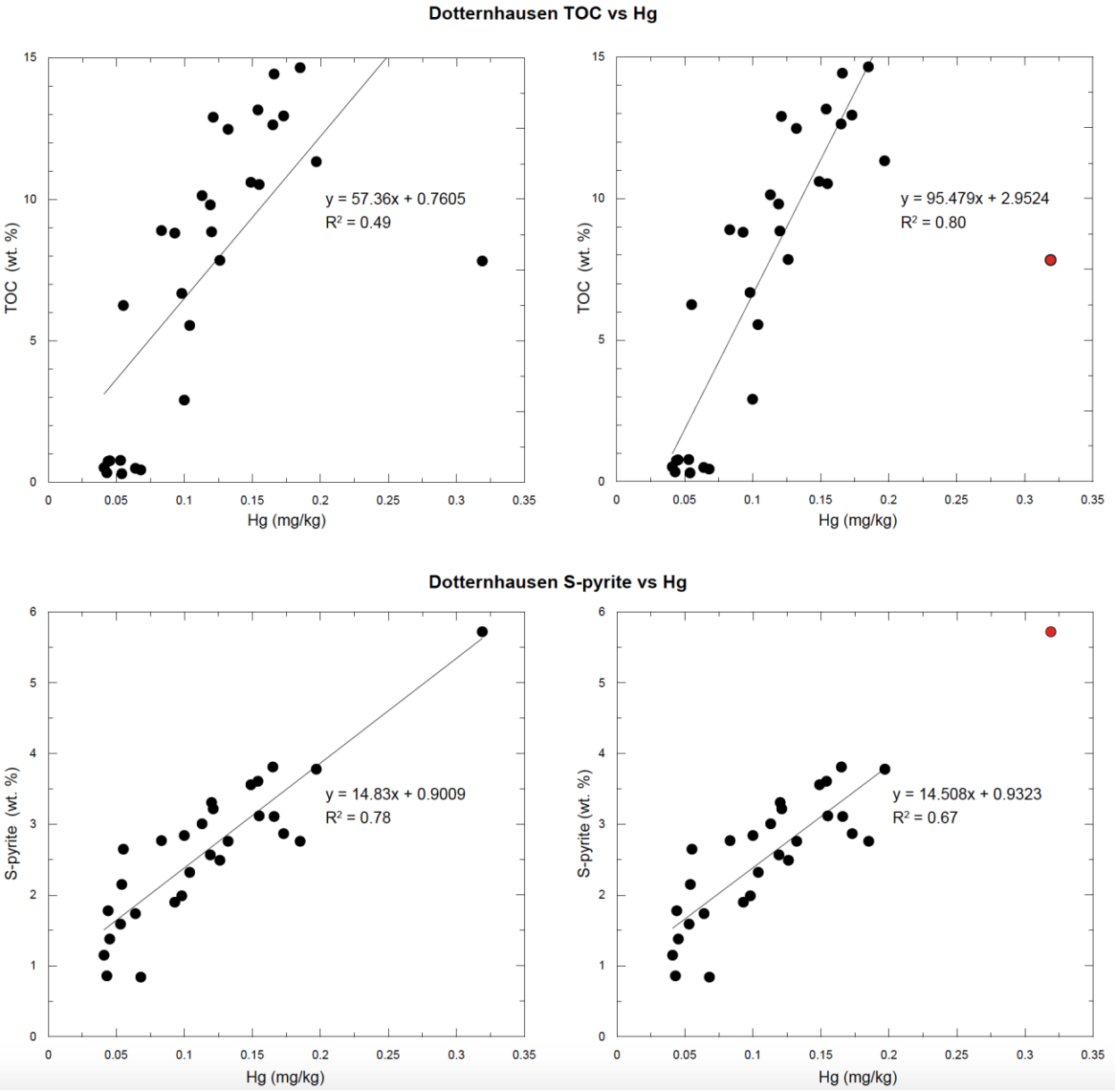

Figure S1. Relationship(s) between Hg and TOC and S-pyrite at Dotternhausen Quarry, Germany. The upper left figure suggests that TOC and Hg are slightly correlated (R^2 = 0.49), but the upper right figure suggests that this correlation is stronger (R^2 = 0.80) when the sample with high pyrite contents (in red) is removed. The lower left figure suggests that pyrite and Hg are strongly correlated to one another stronger (R^2 = 0.78), but this relationship is slightly weaker (R^2 = 0.67) when the sample with high pyrite contents (in red) is removed. The

regression of this relationship, however, is close to approximating the actual sulfur content of this sample. Therefore, the one sample from this section with an *anomalous* Hg and Hg/TOC value during the N-CIE interval (Fig. 4 in main text) is probably controlled by high pyrite contents.

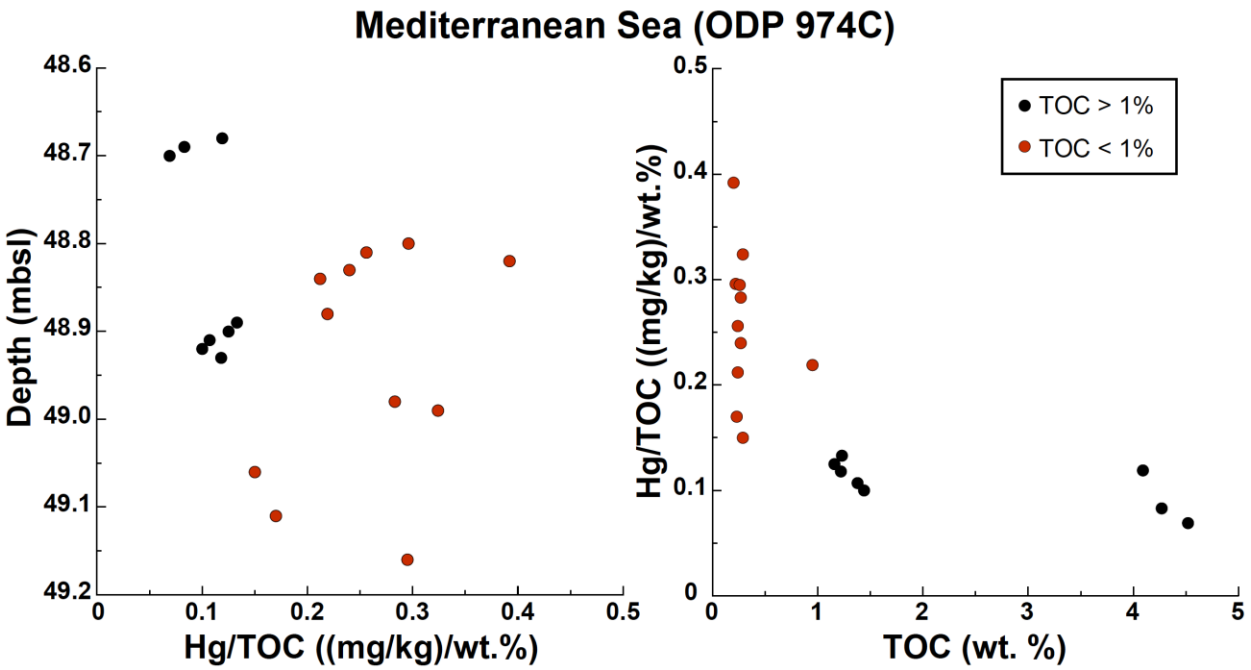

Figure S2. Mercury geochemistry from mid-Pleistocene sediments (ODP Hole 947C) (Gehrke et al., 2009). Black circles represent samples with TOC > 1% (e.g., sapropels) and red circles represent samples with TOC < 1 % (e.g., normal background sedimentation). The Hg/TOC increases associated with the red circles at this site would be interpreted as evidence for increased volcanism if observed in the deep geologic past. Instead, the Hg/TOC anomalies are driven by low TOC values, and these samples were interpreted as being deposited in an oxidizing water column (Gehrke et al., 2009). The samples with elevated Hg contents (i.e., sapropels) were interpreted as being deposited in a reducing/anoxic water column (Gehrke et al., 2009). Therefore, constraining local redox conditions from a study site is paramount when interpreting Hg geochemical records.

Table S2. Ancient Phanerozoic time intervals with reported Hg anomalies.

Age	Reference(s)
Paleocene/Eocene boundary	Jones et al. (in review)
Cretaceous/Paleogene boundary*	Sial et al. (2013, 2014, 2016); Silva et al. (2013); Font et al. (2016, 2018); Percival et al. (2018)
Cenomanian/Turonian boundary† and other Cenomanian events	Scaife et al. (2017); Percival et al. (2018)
Aptian/Albian boundary†	Charbonnier and Föllmi (2017)
Early Cretaceous (Hauterivian through early Aptian)	Charbonnier et al. (2018)
Valanginian/Hauterivian boundary†	Charbonnier et al. (2017)
Pliensbachian/Toarcian boundary and early Toarcian*†	Percival et al. (2015, 2016); Fantasia et al. (2018); *this study*
Triassic/Jurassic boundary*	Thibodeau et al. (2016); Percival et al. (2017)
Permian/Triassic boundary and early Triassic*	Sanei et al. (2012); Grasby et al. (2013, 2016, 2017)
Frasnian/Famennian boundary (Late Devonian)*	Racki et al. (2018)
Ordovician/Silurian boundary*	Jones et al. (2017); Gong et al. (2017)
Middle/Late Ordovician	Liu et al. (2018)

*Mass extinction

† Oceanic anoxic event

REFERENCES CITED IN SUPPLEMENTARY MATERIAL

Charbonnier G, Godet A, Bodin S, Adatte T, Föllmi KB (2018) Mercury anomalies, volcanic pulses, and drowning episodes along the northern Tethyn margin during the latest Hauterivian-earliest Aptian. *Palaeogeogr Palaeoclimatol Palaeoecol* 505:337–350.

Charbonnier G, Morales C, Duchamp-Alphonse S, Westermann S, Adatte T, Föllmi KB (2017) Mercury enrichment indicates volcanic triggering of Valanginian environmental change. *Sci Rep* 7:40808.

Charbonnier G, Föllmi KB (2017) Mercury enrichments support the link between Ontong Java large igneous province activity and oceanic anoxic event 1a. *Geol* 45:63–66.

Fantasia A, et al. (2018) The Toarcian oceanic anoxic event in southwestern Gondwana: an example from the Andean Basin, northern Chile. *J Geol Soc,* doi:10.1144/jgs2018-008.

Font E, Adatte T, Sial AN, de Lacerda LD, Keller G, Punekar J (2016) Mercury anomaly, Deccan volcanism, and the end-Cretaceous mass extinction. *Geol* 44:171–174.

Font E, et al. (2018) Deccan volcanism induced high-stress environment during the Cretaceous-Paleogene transition at Zumaia, Spain: Evidence from magnetic, mineralogical and biostratigraphic records. *Earth Plan Sci Lett* 484:53–66.

Gehrke GE, Blum JD, Meyers PA (2009) The geochemical behavior and isotopic composition of Hg in a mid-Pleistocene western Mediterranean sapropel. *Geochim Cosmo Acta* 73:1651–1665.

Gong Q, et al. (2017) Mercury spikes suggest volcanic driver of Ordovician-Silurian mass extinction. *Sci Rep* 7:5304.

Grasby SE, Beauchamp B, Bond DPG, Wignall PB, Sanei H (2016) Mercury anomalies associated with three extinction events (Capitanian Crisis, Latest Permian Extinction and the

Smithian/Spathian Extinction) in NW Pangea. *Geol Mag* 153:285–297.

Grasby SE, et al. (2017) Isotopic signatures of mercury contamination in latest Permian oceans. *Geol* 45:55–58.

Grasby SE, Sanei H, Beauchamp B, Chen Z (2013) Mercury deposition through the Permo-Triassic Biotic Crisis. *Chem Geol* 351:209–216.

Jones DS, Martini AM, Fike DA, Kaiho KA (2017) A volcanic trigger for the Late Ordovician mass extinction? Mercury data from south China and Laurentia. *Geol* 45:631–634.

Jones MT, et al. (in review) Mercury anomalies across the Palaeocene-Eocene Thermal Maximum, *Clim Past*. doi.org/10.5194/cp-2018-121.

Kondla D, Sanei H, Clarkson CR, Goodarzi F (2017) High resolution characterization of a core from the Lower Jurassic Gordondale Member, Western Canada Sedimentary Basin. *Mar Petr Geol* 83:50–59.

Liu M, Chen D, Zhou X, Yuan W, Jiang M, Liu L (in press) Climatic and oceanic changes during the Middle-Late Ordovician transition in the Tarim Basin, NW China and implications for the Great Ordovician Biodiversification Event. *Palaeogeogr Palaeoclimatol Palaeoecol*. doi: 10.1016/j.palaeo.2018.10.032.

Percival LME, Ruhl M, Hesselbo SP, Jenkyns HC, Mather TA, Whiteside JH (2017) Mercury evidence for pulsed volcanism during the end-Triassic mass extinction. *Proc Natl Acad Sci* 114:7929–7934.

Percival LME, et al. (2015) Globally enhanced mercury deposition during the end-Pliensbachian extinction and Toarcian OAE: A link to the Karoo-Ferrar Large Igneous Province. *Earth Plan Sci Lett* 428:267–280.

Percival LME, et al. (2018) Does Large Igneous Province volcanism always perturb the mercury

cycle? Comparing the records of Oceanic Anoxic Event and the end-Cretaceous to other Mesozoic events. *Amer J Sci* 318:799–860.

Racki G, Rakociński M, Marynowski L, Wignall, PB (2018) Mercury enrichments and the Frasnian-Famennian biotic crisis: A volcanic trigger proved? *Geol* 10.1130/G40233.1.

Riediger CL (1993) Solid bitumen reflectance and Rock-Eval Tmax as maturation indices: an example from the "Nordegg Member", Western Canada Sedimentary Basin. *Int J Coal Geol* 22:295–315.

Riediger CL (2002) Hydrocarbon source rock potential and comments on correlation of the Lower Jurassic Poker Chip Shale, west-central Alberta. *Bull Can Pet Geol* 50:263-276.

Reidiger CL, Fowler MG, Snowdon LR, Goodarzi F, Brooks PW (1990) Source rock analysis of the Lower Jurassic "Nordegg Member" and oil-source rock correlations, northwestern Alberta and northeastern British Columbia. *Bull Can Pet Geol* 38A:236–249.

Sanei H, Grasby SE (2012) Beauchamp B. Latest Permian mercury anomalies. *Geol* 40: 63–66.

Scaife JD, et al. (2017) Sedimentary mercury enrichments as a marker for Submarine Large Igneous Province volcanism? Evidence from the Mid-Cenomanian Event and Oceanic Anoxic Event 2 (Late Cretaceous). *Geochem Geophys Geosys* 18:2017GC007153.

Sial AN, et al. (2013) Mercury as a proxy for volcanic activity during extreme environmental turnover: The Cretaceous-Paleogene transition. *Palaeogeogr Palaeoclimatol Palaeoecol* 387:153–164.

Sial AN, et al. (2014) High-resolution Hg chemostratigraphy: A contribution to the distinction of chemical fingerprints of the Deccan volcanism and Cretaceous-Paleogene Boundary impact event. *Palaeogeogr Palaeoclimatol Palaeoecol* 414:98–115.

Sial AN, et al. (2016) Mercury enrichment and Hg isotopes in Cretaceous-Paleogene boundary

246 successions: Links to volcanism and palaeoenvironmental impacts. *Cret Res* 66:60–81.
247 Silva MVN, Sial AN, Barbosa JA, Ferreira VP, Neumann VH, Lacerda LD (2013) Carbon
248 isotopes, rare-earth elements and mercury geochemistry across the K-T transition of the
249 Paraíba Basin, northeastern Brazil. In: Bojar V, Melinte-Dobrinescu MC, Smit J (Eds.),
250 Isotopic Studies in Cretaceous Research. In: Special Publications, 382. *Geol Soc Lon* 85–104.
251 Them TR II, et al. (2018) Thallium isotopes reveal protracted anoxia during the Toarcian (Early
252 Jurassic) associated with volcanism, carbon burial, and mass extinction. *Proc Natl Acad Sci*
253 115:6596–6601.
254 Thibodeau AM, et al. (2016) Mercury anomalies and the timing of biotic recovery following the
255 end-Triassic mass extinction. *Nat Comm* 7:11147.
256 Wang X, et al. (2018) Mercury anomalies across the end Permian mass extinction in South China
257 from shallow and deep water depositional environments. *Earth Plan Sci Lett* 496:159–167.